Rapid Adaptation of Cardiac Ryanodine Receptors: Modulation by Mg^{2+} and Phosphorylation

Hector H. Valdivia,*† Jack H. Kaplan,‡
Graham C. R. Ellis-Davies,‡ W. Jonathan Lederer

Channel adaptation is a fundamental feature of sarcoplasmic reticulum calcium release channels (called ryanodine receptors, RyRs). It permits successive increases in the intracellular concentration of calcium (Ca^{2+}) to repeatedly but transiently activate channels. Adaptation of RyRs in the absence of magnesium (Mg^{2+}) and adenosine triphosphate is an extremely slow process (taking seconds). Photorelease of Ca^{2+} from nitrophenyl-EGTA, a photolabile Ca^{2+} chelator, demonstrated that RyR adaptation is rapid (milliseconds) in canine heart muscle when physiological Mg^{2+} concentrations are present. Phosphorylation of the RyR by protein kinase A increased the responsiveness of the channel to Ca^{2+} and accelerated the kinetics of adaptation. These properties of the RyR from heart may also be relevant to other cells in which multiple agonist-dependent triggering events regulate cellular functions.

Control of intracellular Ca^{2+} homeostasis is fundamental to the contraction of cardiac muscle. Entry of extracellular Ca^{2+} through voltage-sensitive Ca^{2+} channels triggers the release of Ca^{2+} from the sarcoplasmic reticulum (SR) (*1–3*). This process, Ca^{2+}-induced Ca^{2+} release (CICR), is mediated by the Ca^{2+}-gated Ca^{2+} release channel called the ryanodine receptor (RyR) (*4*). Reconstitution of RyRs in planar lipid bilayers indicates that individual channels are modulated by Ca^{2+} (*5, 6*), Mg^{2+} (*6–8*), adenine nucleotides (*9*), and several protein kinases (*10–12*) under steady-state conditions. However, in the presence of physiological concentrations of Mg^{2+} and adenosine triphosphate (ATP), unphysiologically high concentrations of free Ca^{2+} are required to activate the channel (*7, 13*). This suggests either that a regulatory factor that alters Ca^{2+} sensitivity is lost during RyR reconstitution or that steady-state experiments do not reveal key functional properties of the channel.

The RyR channels have a regulatory mechanism termed adaptation that is triggered when the concentration of Ca^{2+} ($[Ca^{2+}]$) is increased quickly by flash photolysis of caged Ca^{2+} (*14*). Successive increases in $[Ca^{2+}]$ repeatedly open the RyRs which then close (adapt) even though the increased $[Ca^{2+}]$ is maintained. The multiple cycles of opening and closing as the agonist concentration is increased in steps is not predicted by traditional gating models. Adaptation may be the negative feedback mechanism that counters the inherent positive feedback of CICR. However, the rate constant of adaptation in vitro (τ = 1.3 s) is much slower than that of the negative feedback mechanism that controls CICR in vivo ($\tau \sim$ milliseconds). Thus, the physiological relevance of adaptation is unknown. To broaden our understanding of adaptation, we used a caged Ca^{2+} compound, nitrophenyl-EGTA [NP-EGTA (*15*)], that is highly specific for Ca^{2+} and thus permitted us to vary $[Mg^{2+}]$, a factor known to

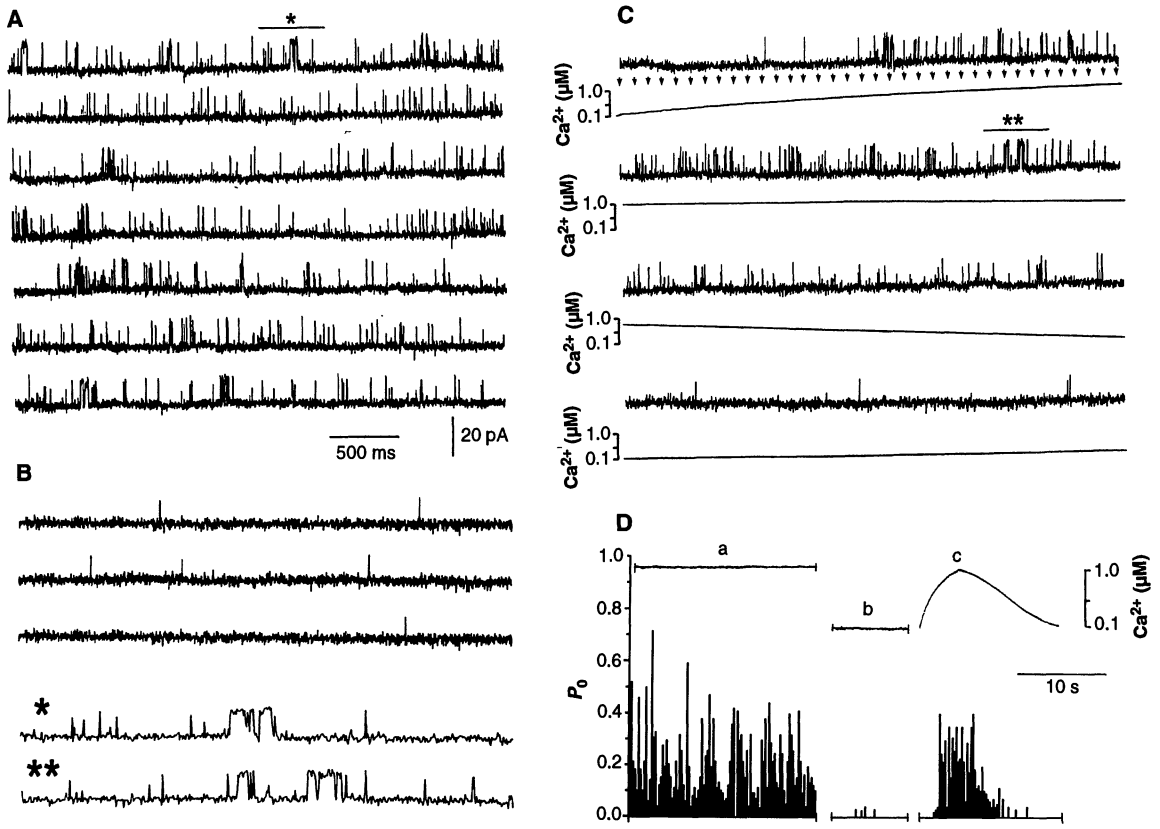

Fig. 1. RyR activity in the presence of a constant $[Ca^{2+}]$ and during a transient increase of the $[Ca^{2+}]$ in the absence of other modulators. Single-channel openings are shown as upward deflections in all figures. The charge carrier is Cs^+ and it flows from the luminal (trans) to the cytosolic (cis) side of the channel. Holding potential = −40 mV. (**A**) Continuous records of stable activity of a single cardiac RyR channel. Concentration of free Ca^{2+} was 1 μM. (**B**) The same channel after buffering $[Ca^{2+}]$ to 100 nM (NP-EGTA, 1.5 mM; $CaCl_2$, 1.02 mM). Traces with asterisks (*) are expansions of segments in (A) and (C) marked with the corresponding symbols. (**C**) Correlation of an increase of RyR activity with a slow increase in the $[Ca^{2+}]$. A train of low-power UV flashes was applied at a frequency of 10 Hz (arrows). The $[Ca^{2+}]$ in the vicinity of the channel was measured with a Ca^{2+} electrode positioned in the path of the light beam, about 0.2 mm in front of the bilayer aperture. (**D**) Relation of RyR activity to $[Ca^{2+}]$. Continuous records in (A), (B), and (C) were divided into intervals of 500 ms; P_o in each interval is plotted as a bar of length 0 to 1. Top traces show the timecourse of the $[Ca^{2+}]$ change near the bilayer surface (not bath $[Ca^{2+}]$). Traces a, b, and c correspond to the calibrated voltage signal from the Ca^{2+} electrode obtained during the recording of single-channel activity shown in panels (A) through (C), respectively.

affect the RyR (6–8).

Individual canine cardiac RyR channels were reconstituted in planar lipid bilayers (*16*), and the concentration of free Ca^{2+} of the solution surrounding the cytosolic face of the channel was buffered to 1 μM by mixing 1 mM NP-EGTA with 0.96 mM $CaCl_2$ (*17*). Under these conditions, long (~2 to 5 ms) and short (≤1 ms) channel openings were evident (Fig. 1A). The probability of the channel being open (P_o) was 0.21 and remained constant throughout the recording period. Decreasing the concentration of free Ca^{2+} to 100 nM by increasing the NP-EGTA:Ca ratio (Fig. 1B) decreased the frequency of long openings and reduced the stationary P_o to <0.01. A slow increase of $[Ca^{2+}]$ in the microenvironment of the channel by application of a train of low-power ultraviolet laser flashes (*18*) slowly increased P_o (Fig. 1C). Channel openings were sparse and brief at first and then became indistinguishable from those in Fig. 1A when $[Ca^{2+}]$ reached ~1 μM. As resting conditions were slowly reestablished, P_o decreased in proportion to the decrease in $[Ca^{2+}]$. Bursts of activity were present only at high $[Ca^{2+}]$ (1 μM) regardless of whether the Ca^{2+} was applied at steady state or by a slow ramp (≤0.25 μM s^{-1}) (Fig. 1D). This indicates that RyR activity is a monotonic function of $[Ca^{2+}]$ if the rate of Ca^{2+} application is adequately slow.

Different RyR kinetics were evoked by a rapid increase of $[Ca^{2+}]$ from 100 nM to 1 μM. RyR activity peaked almost immediately and then spontaneously decayed, even though $[Ca^{2+}]$ remained essentially unchanged (Fig. 2A). The ensemble current generated by summing sweeps of single-channel currents showed that P_o was very high immediately after the flash, and then slowly decayed to a new steady-state about 1.5 s after the flash (Fig. 2D). An exponential fit of the ensemble current showed that the rate of activation [τ_{on} = 1.35 ms (*19*)] and the rate of decay (τ_{adapt} = 1.41 s) were nearly identical to those obtained with the caged Ca^{2+} DM-nitrophen (*14*). After 1 mM Mg^{2+} was added to the cytosolic medium, photolysis increasing $[Ca^{2+}]$ from 100 nM to 1 μM decreased the peak of activation and increased the rate of spontaneous decay (~15-fold faster, τ_{adapt} = 98 ms) (Fig. 2B). The reduced channel conductance (~26% of that in the absence of Mg^{2+}) resulted from Mg^{2+} competing as a current carrier. The long openings observed without Mg^{2+} were virtually absent in the presence of Mg^{2+}, explaining the attenuated P_o. There were several sweeps with few or no openings after the flash, which also accounted for the depressed peak of the ensemble current. Open events were rarely observed by the end of the sweep. A larger increase in $[Ca^{2+}]$ to 10 μM was required to achieve a peak of activity similar to that seen in the absence of Mg^{2+} (Fig. 2C).

The larger increase in the $[Ca^{2+}]$ increased the rate of openings, but the rate of decay was still fast (τ_{adapt} = 168 ms). Thus, physiological $[Mg^{2+}]$ shifted the threshold of RyR activation by Ca^{2+} to a higher $[Ca^{2+}]$ and accelerated adaptation of the receptor to a rate comparable with that seen for the decay of the transient increase in intracellular $[Ca^{2+}]$ in intact cells [half-life, $t_{1/2}$, of ~150 ms (*1–3*)]. With an increase in the final $[Ca^{2+}]$ step to 10 μM, the peak P_o was similar to that thought to occur in vivo (*20*). The $[Ca^{2+}]$ needed to more fully activate the RyR is higher than the global $[Ca^{2+}]$ reached in a heart cell at the peak of the contraction. Hence, high local $[Ca^{2+}]$ [which may occur when dihydropyridine-sensitive Ca^{2+} channels on the sarcolemma open in close proximity to the RyR (*1, 3, 21*)] is required to evoke substantial Ca^{2+} release.

We applied a standard increase in $[Ca^{2+}]$ from 0.1 to 10 μM and measured the effect of various $[Mg^{2+}]$ on the kinetics of the RyR (Fig. 3). Ensemble currents were constructed by summing single-channel sweeps obtained in the absence and the presence of Mg^{2+} (Fig. 3A). In the absence of Mg^{2+}, peak P_o reached ~1.0, suggesting that 10 μM Ca^{2+} alone was sufficient to maximally activate the channel. However, the rate of decay was slow (τ_{adapt} = 1.35 s), and the P_o at the end of the sweep was still high. At the maximal $[Mg^{2+}]$ tested (3 mM), the peak P_o and plateau P_o decreased to 0.42 and 0.04, respectively. Thus, the transient and steady-state activities of the RyR are inversely related to the $[Mg^{2+}]$. The rate of adaptation was increased by Mg^{2+}, with a concentration of ~100 μM yielding the half-maximal effect (Fig. 3B) and a Hill coefficient of 1.1, suggesting that Mg^{2+} probably acted at a single binding site to produce this effect. Half-maximal inhibition of CICR by Mg^{2+} in skeletal muscle occurs at a concentration of 230 μM (*22*); however, skeletal RyRs are known to be more sensitive to blockade by Mg^{2+} (*23*). Thus, adaptation may be promoted by Mg^{2+} in both heart and skeletal muscle.

Cardiac RyRs are important substrates for the adenosine 3′,5′-monophosphate (cAMP)–dependent protein kinase A(PKA) (*10, 11*). In intact ventricular myocytes, PKA increases the amplitude and the rate of decay of the intracellular Ca^{2+} transient (*24*). We tested the effect of the catalytic subunit of PKA on RyR activity (*25*). At a constant bath $[Ca^{2+}]$ of 10 μM, PKA (1 μg/ml) decreased [^{3}H]ryanodine binding to cardiac SR vesicles by

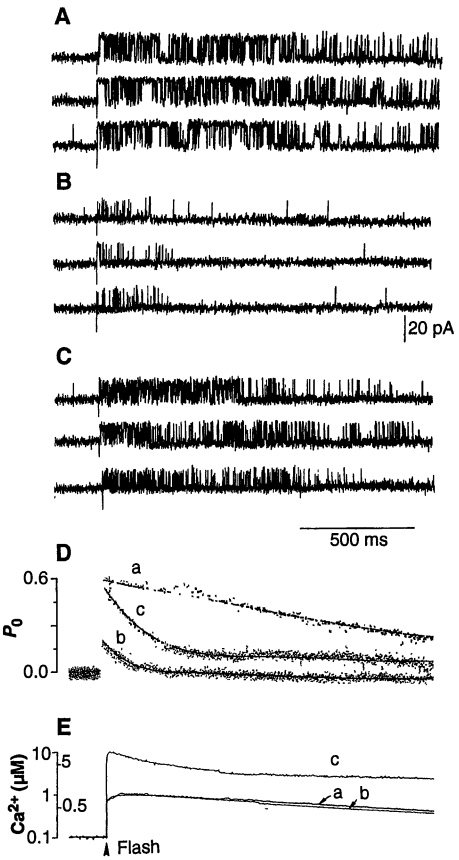

Fig. 2. Activation of a RyR by very fast changes of the $[Ca^{2+}]$. The resting $[Ca^{2+}]$ was 0.1 μM in all traces. Calibrated step increases of $[Ca^{2+}]$ were achieved by varying the power output of the laser apparatus [Q-switch mode (*18*)]. Resting conditions were reestablished by stirring the cis (that is, cytoplasmic) chamber. The RyR openings were elicited by fast increases of $[Ca^{2+}]$ to 1 μM (**A** and **B**) or to 10 μM (**C**) produced by single ~7-ns light pulses. A 1 mM concentration of free Mg^{2+} (1.02 mM $MgCl_2$) was present in (B) and (C). Traces in all panels were recorded from the same channel. (**D**) Ensemble currents were generated by the sum of data sweeps (curve a, 18 sweeps; curve b, 16 sweeps; and curve c, 23 sweeps) and correspond to the single-channel records shown in (A), (B), and (C), respectively. The time course of the spontaneous decay of activity was best fit by a single exponential function. The time constants of adaptation were (curve a) 1.41 s, (curve b) 98 ms, and (curve c) 168 ms. The means ± SD for n = 4 experiments were (curve a) 1.52 ± 0.2 s, (curve b) 107 ± 16 ms, and (curve c) 154 ± 27 ms. (**E**) Amplitude and time course of the change in $[Ca^{2+}]$ in the microenvironment of the channel as measured simultaneously with a Ca^{2+} electrode during the course of the experiment.

H. H. Valdivia and W. J. Lederer, Department of Physiology and Medical Biotechnology Center, University of Maryland Medical School, Baltimore, MD 21201, USA.
J. H. Kaplan and G. C. R. Ellis-Davies, Department of Physiology, University of Pennsylvania, Philadelphia, PA 19104, USA.

*To whom correspondence should be addressed.
†Present address: Department of Physiology, University of Wisconsin, 1300 University Avenue, Madison, WI 53706, USA.
‡Present address: Department of Biochemistry and Molecular Biology, Oregon Health Sciences University, Portland, OR 97201, USA.

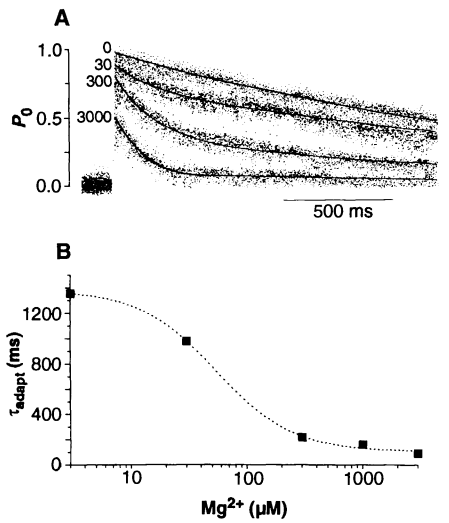

Fig. 3. Effect of Mg^{2+} on the peak, plateau, and rate of adaptation of RyR activity. (**A**) Ensemble currents obtained in the presence of the indicated [Mg^{2+}] (0 to 3000 μM). Photolysis of caged Ca^{2+} increased [Ca^{2+}] from 0.1 to 10 μM in all cases. The number of data sweeps at each [Mg^{2+}], obtained from two independent experiments, were (0 μM Mg^{2+}) 49, (30 μM Mg^{2+}) 38, (300 μM Mg^{2+}) 28, and (3000 μM Mg^{2+}) 46. (**B**) The rate constant of spontaneous decay of RyR activity, τ_{adapt}, is plotted against [Mg^{2+}]. Data points were fitted with the equation $\tau_{adapt} = \tau_{adapt}max/[1 + ([Mg^{2+}]/K_{0.5})^n]$ where $\tau_{adapt}max$ is the rate constant of adaptation in the absence of Mg^{2+}, $K_{0.5}$ is the half-maximal [Mg^{2+}] necessary to accelerate adaptation, and n is the Hill number.

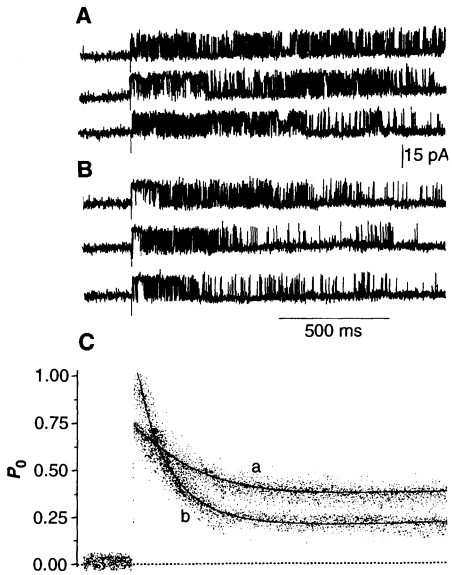

Fig. 4. Modification of RyR kinetics by PKA-dependent phosphorylation. Single laser pulses produced a photorelease-dependent increase in [Ca^{2+}] from 0.1 to 10 μM in all panels. (**A**) Activation of a single RyR in the presence of 3 mM ATP and 4 mM $MgCl_2$ (a concentration of free Mg^{2+} of ~1 mM). (**B**) Representative traces of the same channel taken ~1 min after addition of the catalytic subunit (1 μg/ml) of PKA to the cytosolic solution (*25*). (**C**) Ensemble currents generated by summing 17 sweeps (curve a) and 21 sweeps (curve b) corresponding to the single-channel traces shown in panels (A) and (B), respectively. In each case, activity peaked within 5 ms after photolysis and then spontaneously decayed with a τ_{adapt} = 187 ms (curve a) or 106 ms (curve b).

34 ± 8% (mean ± SD, n = 4) and steady-state P_o of cardiac RyR by 26 ± 9%. This effect would appear to be at odds with the effect of activation of PKA in cells (*24*). Because differences in single RyR responses to [Ca^{2+}] and cellular responses to intracellular [Ca^{2+}] reside in the kinetics of the responses, we applied fast Ca^{2+} steps by photorelease of Ca^{2+} and examined the transient response of the RyR before and after phosphorylation by PKA (Fig. 4).

In the presence of 3 mM ATP and 4 mM $MgCl_2$ [a concentration of free Mg^{2+} of ~1 mM (Fig. 4A)], an increase in [Ca^{2+}] to 10 μM increased the peak P_o determined from ensemble currents from <0.01 to 0.73. Adaptation of the channel led to a plateau P_o of 0.38 with a rate constant of decay of 187 ms (Fig. 4C). In contrast, when an increase in [Ca^{2+}] to 10 μM was triggered 1 min after the addition of PKA (1 μg/ml) to the cytosolic side of the channel (Fig. 4B), peak P_o of the same channel consistently increased from <0.01 to ~1.0. Adaptation of the channel led to a new steady-state P_o of 0.21 with a rate constant of decay of 106 ms (Fig. 4C). A similar concentration of PKA failed to induce the kinetic changes described above when ATP was replaced with the nonhydrolyzable analog β,γ-methyleneadenosine 5′-triphosphate (AMP-PCP) (*26*). Thus, we interpret the kinetic changes induced by PKA as being the result of phosphorylation of the RyR or of a closely associated regulatory protein that incorporates in the bilayer with the RyR. The lower steady-state activity caused by PKA explains the modest inhibitory effect of PKA in [^{3}H]ryanodine binding and lipid bilayer experiments at constant [Ca^{2+}]. The increased peak of activity and the faster rate of decay induced by PKA may enable RyRs to increase their sensitivity to a triggering Ca^{2+} current and to adapt quickly, thus permitting faster availability of RyRs for subsequent triggers, features known to occur in heart muscle treated with β-adrenergic agonists.

Channel adaptation appears to be a physiologically important property of the cardiac RyR. A normal intracellular [Mg^{2+}] was required to achieve the appropriate kinetic responsiveness in bilayer experiments that is seen in intact heart cells. Additionally, the lower sensitivity of the RyR to Ca^{2+} observed in the presence of Mg^{2+} is consistent with (i) the low sensitivity of response to a global change of [Ca^{2+}] seen in intact cells (*1*, *3*) and (ii) the absence of self-propagating CICR in normal cells despite spontaneous or photolysis-generated increases in [Ca^{2+}] (*3*, *27*). Adaptation may function in modulating CICR and intracellular Ca^{2+} signaling in many cell types that use Ca^{2+} release channels of the RyR and inositol triphosphate receptor superfamily to provide primary or amplified secondary intracellular Ca^{2+} signals. The increased sensitivity of the RyR to a [Ca^{2+}] step, the faster adaptation, and the lower steady-state sensitivity to [Ca^{2+}] after phosphorylation by PKA reveals a potential mechanism by which multiple regulatory pathways may modulate the complex time course of Ca^{2+} release in the heart.

REFERENCES AND NOTES

1. E. Niggli and W. J. Lederer, *Science* **250**, 565 (1990).
2. M. Cannell, J. Berlin, W. J. Lederer, *ibid.* **238**, 1419 (1987); J. Beuckelmann and W. Wier, *J. Physiol. (London)* **405**, 233 (1988); L. Cleemann and M. Morad, *ibid.* **432**, 283 (1991).
3. H. Cheng, W. J. Lederer, M. B. Cannell, *Science* **262**, 740 (1993).
4. M. Inui *et al.*, *J. Biol. Chem.* **262**, 1740 (1987); T. Imagawa *et al.*, *ibid.*, p. 16636; F. A. Lai *et al.*, *Nature* **331**, 315 (1988).
5. J. S. Smith *et al.*, *J. Gen. Physiol.* **92**, 1 (1988).
6. A. Tinker and A. J. Williams, *ibid.* **100**, 479 (1992).
7. G. Meissner and J. S. Anderson, *J. Biol. Chem.* **262**, 3065 (1987).
8. S. R. M. Holmberg and A. J. Williams, *Biochim. Biophys. Acta* **1022**, 187 (1990).
9. G. Meissner, *J. Biol. Chem.* **259**, 2365 (1984).
10. D. Witcher *et al.*, *ibid.* **266**, 11144 (1991).
11. T. Takasago, T. Imagawa, M. Shigekawa, *J. Biochem. (Tokyo)* **106**, 872 (1989).
12. M. Strand, C. Louis, J. Mickelson, *Biochim. Biophys. Acta* **1175**, 319 (1993).
13. I. N. Pessah, R. A. Stambuk, J. E. Casida, *Mol. Pharmacol.* **31**, 232 (1987).
14. S. Györke and M. Fill, *Science* **260**, 807 (1993).
15. G. C. R. Ellis-Davies and J. H. Kaplan, *Proc. Natl. Acad. Sci. U.S.A.* **91**, 187 (1994).
16. Heavy SR-enriched microsomes were isolated by differential centrifugation from dog hearts by a modification of the method of Tate [C. A. Tate *et al.*, *J. Biol. Chem.* **260**, 9618 (1985)]. The fusion of microsomes into planar lipid bilayers and analysis of single-channel kinetics were done as described (*28*, *29*). Bilayers were composed of 50% phosphatidylethanolamine and 50% phosphatidylserine (25 mg/ml in *n*-decane). The cis solution was 300 mM $CsCH_3SO_3$, 50 mM Hepes (pH 7.4), and NP-EGTA:Ca^{2+} admixtures as specified in the text. The trans solution was 50 mM $CsCH_3SO_3$ before SR fusion and 300 mM after fusion. We used Cs^+, instead of Ca^{2+}, as the charge carrier to precisely control [Ca^{2+}] around the channel, to increase the signal-to-noise ratio (unitary conductance to Cs^+/unitary conductance to Ca^{2+} ~ 2), and to block K^+ channels of the SR (*5*). The number and orientation of channels in the bilayer was determined under optimal steady-state conditions before the beginning of the experiment.
17. The dissociation constant (K_d) of the unphotolyzed NP-EGTA–Ca^{2+} complex in isotonic solutions at pH 7.5 is 26 nM. Under the same conditions, K_d of the NP-EGTA–Mg^{2+} complex is 9 mM (*15*). Therefore, addition of 1 mM $MgCl_2$ to solutions containing 1 to 1.5 mM NP-EGTA and Ca^{2+} buffered to 100 nM was expected to produce only a small (~5%) alteration of the free Ca^{2+} concentration. Before flash experiments, the concentration of free Ca^{2+} was monitored with a Ca^{2+} electrode in the bath, and changes brought about by the addition of Mg^{2+} or repetitive

flashes were compensated for with fresh NP-EGTA and $CaCl_2$.

18. The time course and magnitude of the change in $[Ca^{2+}]$ could be modified by varying the frequency and the discharge energy of the Q-switched, frequency-tripled, neodymium-doped:yttrium-aluminum-garnet (Nd:YAG) laser (model GCR-18, Spectra-Physics, Mountain View, CA). Ultraviolet light (352 nm) from the laser was separated from the 1064 and 532 lines with three dichroic mirrors (350 to 360 nm), collected by a convergent mirror, and focused onto the polished aperture of a ~400-μm outer diameter, fused-silica light guide (Fiberguide, Stirling, NJ). The end of the light guide was positioned with a micromanipulator ~400 μm in front of the bilayer aperture to photolyze the caged Ca^{2+} in a cylinder-shaped region between the end of the fiber optic light guide and the bilayer cup. Slow changes in $[Ca^{2+}]$ ("Ca^{2+} ramps") were produced by setting a low output energy of the flash lamp (5 to 15 mJ) and pulsing the laser at 10 Hz. Fast $[Ca^{2+}]$ changes (~100 μs, the rate time constant of Ca^{2+} release by NP-EGTA) were produced by 50- to 80-mJ single flashes. All flashes were ~7 ns in duration. We measured the local changes in $[Ca^{2+}]$ by two methods. In one case, small (50- to 70-μm tip diameter) plastic pipettes were filled with a Ca^{2+} ionophore resin (catalogue no. 21199, Fluka Chemical, New York, NY) and positioned in the path of the light beam, ~200 μm away from the bilayer surface. In the second case, the bilayer aperture was filled with the Ca^{2+} ionophore resin as described (*14*), and the change in $[Ca^{2+}]$ was determined in separate experiments. Both methods yielded very similar results.
19. H. H. Valdivia, J. H. Kaplan, G. C. R. Ellis-Davies, W. J. Lederer, unpublished data.
20. D. Bers, *Am J. Physiol.* **256**, C109 (1989); I. Baró *et al.*, *J. Physiol. (London)* **465**, 21 (1993).
21. W. J. Lederer *et al.*, *Science* **251**, 1371 (1990).
22. P. J. O'Brien, *Can. J. Vet. Res.* **50**, 318 (1986).
23. E. Rousseau *et al.*, *Biophys. J.* **50**, 1009 (1986).
24. G. Callewaert, L. Cleeman, M. Morad, *Proc. Natl. Acad. Sci. U.S.A.* **85**, 2009 (1988); H. A. Spurgeon *et al.*, *Am. J. Physiol.* **258**, H574 (1990).
25. The catalytic subunit of PKA (Sigma Chemical, St. Louis, MO) was activated before use with 0.5 M dithiothreitol (DTT) for 30 min at 32°C and dialyzed for 4 hours at 4°C against the cis solution with 1 mM DTT (*30*). PKA was added directly to the cis solution supplemented with 1 mM MgATP, and the RyR activity was recorded 1 to 2 min after addition. The binding of $[^3H]$ryanodine (7 nM) to porcine cardiac SR vesicles (0.3 mg/ml) was done for 90 min at 36°C in 0.2 M KCl, 10 mM Na-Pipes (pH 7.2), 1 mM MgATP, and 10 μM $CaCl_2$, as described (*28, 29*).
26. Similar to ATP, the addition of 3 mM AMP-PCP to the cis (cytosolic) side of the channel increased the peak P_o and the plateau P_o of single RyRs activated by a fast change in $[Ca^{2+}]$ from 0.1 to 10 μM in the presence of 4 mM $MgCl_2$. This suggested that AMP-PCP was as effective as ATP to directly activate RyRs (*9*), decrease the concentration of free Mg^{2+}, or both. However, in two experiments, AMP-PCP–treated RyRs did not change significantly peak P_o (0.68, 0.71), τ_{adapt} (196, 173 ms), and plateau P_o (0.29, 0.32) when recorded in the absence and the presence, respectively, of PKA (1 μg/ml).
27. S. C. O'Neill, J. G. Mill, D. Eisner, *Am. J. Physiol.* **258**, C1165 (1990).
28. H. H. Valdivia *et al.*, *J. Biol. Chem.* **266**, 19135 (1991).
29. H. H. Valdivia, M. Kirby, W. J. Lederer, R. Coronado, *Proc. Natl. Acad. Sci. U.S.A.* **89**, 12185 (1992).
30. A. Yatani *et al.*, *J. Biol. Chem.* **263**, 9887 (1988).

31. We thank M. Fill for his help with the experimental setup modeled on his own (*14*), M. Kirby for help with the Ca^{2+} electrode, and M. Fill, G. Meissner, I. Pessah, and E. Ríos for critical comments on this manuscript. Supported by a Grant-in-Aid from the American Heart Association (AHA) to H.H.V., NIH grants HL36974 and HL25675 (to W.J.L.) and HL30315 and GM39500 (to J.H.K.). H.H.V. is a recipient of a Minority Scientist Development Award from the AHA.

13 September 1994; accepted 13 December 1994

Altered Cytokine Export and Apoptosis in Mice Deficient in Interleukin-1β Converting Enzyme

Keisuke Kuida, Judith A. Lippke, George Ku, Matthew W. Harding, David J. Livingston, Michael S.-S. Su,* Richard A. Flavell*

The interleukin-1β (IL-1β) converting enzyme (ICE) processes the inactive IL-1β precursor to the proinflammatory cytokine. Adherent monocytes from mice harboring a disrupted ICE gene ($ICE^{-/-}$) did not export IL-1β or interleukin-1α (IL-1α) after stimulation with lipopolysaccharide. Export of tumor necrosis factor–α and interleukin-6 (IL-6) from these cells was also diminished. Thymocytes from $ICE^{-/-}$ mice were sensitive to apoptosis induced by dexamethasone or ionizing radiation, but were resistant to apoptosis induced by Fas antibody. Despite this defect in apoptosis, $ICE^{-/-}$ mice proceed normally through development.

The cytokine IL-1β plays a pivotal role in acute and chronic inflammation, bone resorption, myelogenous leukemia, and other pathological processes (*1*). IL-1β is synthesized as a 31-kD precursor devoid of a conventional signal sequence (*2*) and is processed to its proinflammatory 17-kD form by ICE, a cysteine protease with substrate cleavage specificity for Asp-X (*3*). ICE itself is synthesized principally in monocytes as an inactive proenzyme that autoprocesses to an active tetramer composed of two 10-kD and two 20-kD subunits (*4, 5*). With the cloning of the *Caenorhabditis elegans* cell death gene *ced-3* (*6*), ICE was recognized to be a member of a new subfamily of cysteine proteases. ICE and CED-3 show only 28% sequence conservation overall, but their active site residues are completely conserved (*5, 6*).

Although the physiological functions of the mammalian ICE homologs are unknown, overexpression of ICE and ICE homologs in transfected cell lines induces apoptosis (*7, 8*). This effect is reduced when ICE is coexpressed with Bcl-2, a mammalian oncogenic protein that is a general suppressor of apoptosis (*9*). Further, transfection of chicken dorsal ganglion cells with CrmA, a serpin-like inhibitor of ICE (*10*) and potentially of ICE homologs, protects these cells from apoptosis induced by depletion of nerve growth factor (*11*).

To probe the physiological functions of ICE, we disrupted the murine ICE gene in D3 embryonic stem (ES) cells by replacing part of exons 6 and 7 (Fig. 1A) with a neomycin resistance gene cassette (*12, 13*). Chimeric mice were obtained by injection of mutant ES cells into C57BL/6 blastocysts, and the chimeric males were mated with C57BL/6 mice. Interbreeding of the heterozygous mice generated the expected mendelian 1:2:1 ratio of wild-type ($ICE^{+/+}$), heterozygous ($ICE^{+/-}$), and homozygous ($ICE^{-/-}$) mutant mice. Homozygous mice with two copies of the disrupted ICE gene

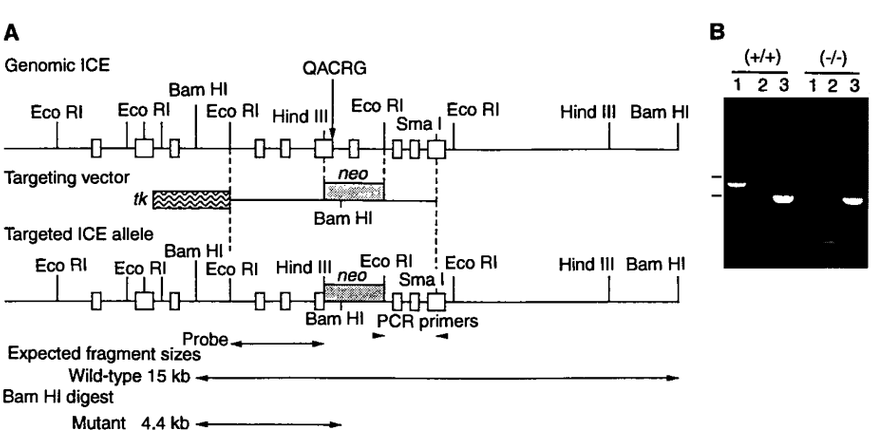

Fig. 1. Disruption of the murine ICE gene by homologous recombination (*13*). (**A**) Restriction maps of the murine ICE locus, the targeting vector, and the mutant ICE locus. (**B**) RT-PCR analysis of mRNA from $ICE^{+/+}$ and $ICE^{-/-}$ mice with oligonucleotide primers (*13*) specific for wild-type ICE cDNA (1), mutated ICE cDNA (2), and β-actin cDNA (3). The lines on the left indicate the positions of 984-bp (upper) and 738-bp (lower) markers.